Surface-Enhanced Raman Scattering in Local Optical Fields of Silver and Gold Nanoaggregates—From Single-Molecule Raman Spectroscopy to Ultrasensitive Probing in Live Cells

KATRIN KNEIPP,*,†,‡ HARALD KNEIPP,† AND JANINA KNEIPP†,§

Wellman Center for Photomedicine, Harvard University Medical School, Boston Massachusetts 02114, Harvard-MIT Division of Health Sciences and Technology, Cambridge, Massachusetts 02139, and FG I.3 Structure Analyses, Federal Institute for Materials Research and Testing, D 12489 Berlin, Germany

Received November 29, 2005

ABSTRACT

This Account discusses surface-enhanced Raman scattering at extremely high enhancement levels that can occur for molecules attached to silver and gold nanoclusters. Strongly enhanced and highly confined local optical fields enable surface-enhanced Stokes and anti-Stokes Raman spectroscopy of single molecules even under nonresonant excitation conditions as well as extremely large effective cross sections in two-photon excited Raman spectroscopy. The ability for very sensitive and spatially confined molecular structural probing makes gold and silver nanoclusters very promising tools for studies of small structures in biological materials, such as cellular compartments.

Introduction

Characterizing the chemical structure of a single molecule and monitoring structural changes at the single-molecule level belong to the most challenging goals in chemistry. High-throughput structurally selective detection and counting single molecules represents the ultimate limit in chemical analysis. Molecular vibrations and therefore molecular structure can be probed by the inelastic Raman scattering process. Depending on the excitation frequency, Raman scattered light can be observed in the UV to near-infrared frequency range. Raman spectroscopy provides a unique approach for solving analytical problems. However, Raman scattering has an extremely small cross section, typically $\sim 10^{-30}$ to 10^{-25} cm^2 per molecule, with the larger values occurring only under favorable resonance Raman conditions. The small Raman cross sections require a large number of analyte molecules to achieve adequate conversion rates from excitation laser photons to Raman photons. Therefore, usually, Raman spectroscopy has been considered a technique for structural analysis, rather than a method for ultrasensitive trace detection or even as tool at the level of single molecules. However, Raman scattering literally appears in a new light when it takes place in the local optical fields of metal nanostructures. The favorable optical properties of these metal nanostructures, based on their surface plasmon polaritons, provide the key effect for the observation of enhanced Raman signals for molecules attached to them, the effect of surface-enhanced Raman scattering (SERS). SERS at extremely high enhancement levels transforms Raman spectroscopy from a structural analytical tool to a structurally sensitive single-molecule and nanoscale probe. At present, SERS is the only way to detect a single molecule and simultaneously probe its chemical structure.

In this Account, we discuss the strongly enhanced Raman scattering signals that occur when the target molecules are attached to silver and gold nanoclusters. In particular, we elucidate why these nanostructures work so well for single-molecule Raman spectroscopy. In addition to linear SERS spectroscopy, we will also consider nonlinear surface-enhanced Raman scattering, because two-photon excited processes benefit particularly from enhanced local optical fields. In the last section, we discuss the application of gold nanoaggregates as SERS nanosensors enabling ultrasensitive targeted Raman probing in live cells.

The Trail to Single-Molecule Raman Spectroscopy

In 1977, Van Duyne and Jeanmaire and, independently, Albrecht and Creighton confirmed the 1974 experiments on enhanced Raman signals from pyridine on a rough silver electrode,[1] and they concluded that the enormously strong Raman signal measured must be caused by true enhancement of the Raman scattering efficiency itself.[2,3] Enhanced Raman signals measured from pyridine in aqueous silver and gold colloidal solutions[4] showed that SERS is not as much a surface effect as it is a nanostructure effect and provided the first clear demonstration of the important role of plasmon resonances and the elec-

Katrin Kneipp received her Diplom and Ph.D. degree in Physics and Dr.sc. in Physical Chemistry from Friedrich Schiller University in Jena, Germany. Her current research interests at Harvard Medical School include single-molecule and nanoscale spectroscopies and their broad interdisciplinary applications.

Harald Kneipp received his Diplom in Physics from Friedrich Schiller University in Jena and a Ph.D. degree in Physics from the Academy of Sciences in Berlin. He conducted research in the fields of plasma physics, nonlinear optics, and laser physics and development. His current interests include applications of lasers and optical spectroscopy at the frontiers of science and medicine.

Janina Kneipp received her Diplom in Biology and after thesis work at Robert-Koch-Institut a Ph.D. from Free University Berlin in 2002. During her postdoctoral studies, she worked at Princeton University's Chemistry Department and conducted research at Harvard Medical School. Her research at the Federal Institute for Materials Research and Testing, Berlin, is focused on the development of novel sensitive vibrational spectroscopic methods to investigate small-scale complex biomaterials.

* Corresponding author. E-mail: kneipp@usa.net. Phone: +1-617-724-2095.
† Harvard University Medical School.
‡ Harvard-MIT Division of Health Sciences and Technology.
§ Federal Institute for Materials Research and Testing.

10.1021/ar050107x CCC: $33.50
Published on Web 04/26/2006

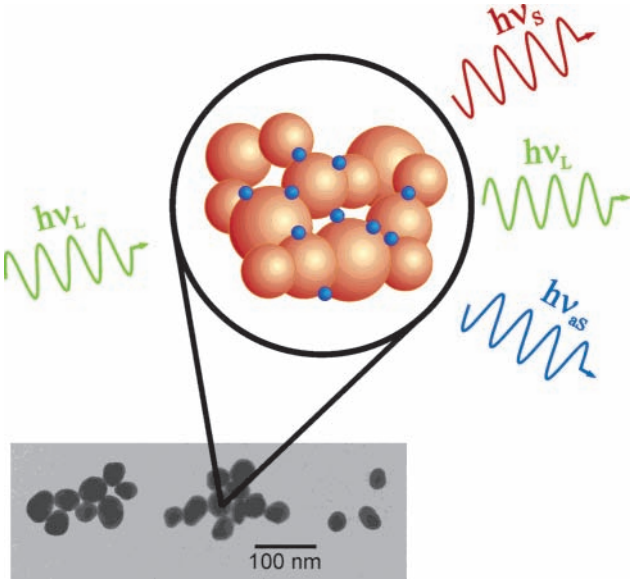

FIGURE 1. Surface-enhanced Raman scattering.

tromagnetic field enhancement in SERS.[5] But there was also experimental evidence that different effects must contribute to the observed enhanced Raman signal, including so-called chemical effects, where enhancement mechanisms for the Raman signal can be understood in terms of various possible electronic interactions between molecule and metal.[6,7] For an overview on surface-enhanced Raman scattering see refs 6 and 8−12.

Figure 1 shows a schematic of surface-enhanced Raman scattering. Molecules (blue dots) are attached to metal nanoparticles (orange balls); for an example, see the electron micrograph of colloidal gold particles. The SERS Stokes signal, $P^{SERS}(\nu_S)$, can be estimated according to eq 1.[10]

$$P^{SERS}(\nu_S) = N\sigma^{R}_{ads}|A(\nu_L)|^2|A(\nu_S)|^2 I(\nu_L) \qquad (1)$$

with $I(\nu_L)$ = excitation laser intensity, σ^{R}_{ads} = Raman cross section of the adsorbed molecule, possibly increased due to chemical enhancement, N = number of molecules involved in the SERS process, and $A(\nu_L)$ and $A(\nu_S)$ = field enhancement factors (laser and Raman). Equation 1 shows that the electromagnetic SERS enhancement factor is determined by the fourth power of the field enhancement in the local optical fields of the metal nanoparticles.

SERS enhancement factors were estimated by comparing surface-enhanced Raman signals and normal Raman scattering or fluorescence, taking into account the different concentrations of molecules contributing to the observed signals. The estimated enhancement factors for the Raman signal started with modest factors of 10^3−10^5 observed in the initial experiments. Many authors could later observe enhancement factors of 10^{10}−10^{11} for dye molecules in surface-enhanced resonance Raman scattering.[13−15] At that time, SERRS spectra were measured from ~100 rhodamine 6G molecules in aggregated silver colloidal solution and suggested that single-molecule

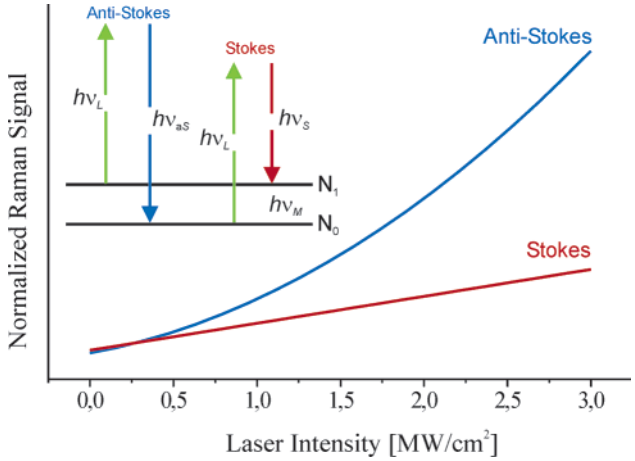

FIGURE 2. Anti-Stokes and Stokes signal vs excitation intensity measured from crystal violet attached to silver nanoclusters.

Raman spectroscopy should be possible by further experimental improvement for SERRS.[15,16]

In 1995, a new approach for determining effective SERS cross sections using anti-Stokes to Stokes signal ratios identified unexpectedly large nonresonant SERS cross sections on the order of at least 10^{-16} cm^2 per molecule, which corresponds to enhancement factors of about 14 orders of magnitude.[17] Such numbers exceeded all previous estimates of SERS enhancement factors by 2−3 orders of magnitude. Assuming consistency of the enhancement factors with the observed scattering signal, one has to conclude that a very small number of molecules in the SERS sample are involved in the SERS process at such a high enhancement level. On the basis of this finding, we drastically reduced the number of molecules in the probed volume and measured Raman spectra from single molecules using near-infrared excitation nonresonant to the electronic transitions in the target molecules.[18−20] Nie and Emory improved the surface-enhanced resonance Raman experiments on rhodamine 6G to single-molecule sensitivity.[21]

Single-Molecule Raman Scattering in Local Optical Fields of Silver and Gold Nanoaggregates

Effective Raman Cross Section and Enhancement Factors. SERS enhancement factors were underestimated for many years when they were inferred from a comparison between surface-enhanced Raman signals and normal Raman scattering or fluorescence. The main reason for this general mistake was the assumption that all molecules in a SERS experiment contribute to the observed SERS signal. To avoid this problem, we applied a different approach, in which both surface-enhanced Stokes *and* anti-Stokes Raman scattering were used to extract information on the effective SERS cross section from experimentally observed population pumping to the first excited vibrational level due to a very strong Raman process.[17]

Figure 2 illustrates Stokes and anti-Stokes scattering in a molecular-level scheme. Population and depopulation of the first excited vibrational level by Raman Stokes and

anti-Stokes transitions can be described by the rate equation

$$\frac{dN_1}{dt} = (N_0 - N_1)\sigma^{SERS} n_L - \frac{N_1}{\tau_1} \quad (2)$$

Simple equations for the anti-Stokes (eq 3a) and Stokes signals (eq 3b) can be derived from eq 2 assuming steady state and weak saturation ($\exp(-h\nu_M/(kT)) \leq \sigma_S^{SERS}\tau_1 n_L \ll 1$). Under weak saturation conditions, a continuous wave (cw) laser-excited Raman process populates the first excited vibrational state comparably or higher than the Boltzmann population but still far away from approaching equilibrium population between N_0 and N_1.

$$P_{aS}^{SERS} = (N_0\, e^{-h\nu_M/(kT)} + N_0\sigma^{SERS}\tau_1 n_L)\sigma^{SERS} n_L \quad (3a)$$

$$P_S^{SERS} = N_0\sigma^{SERS} n_L \quad (3b)$$

with σ^{SERS} = effective SERS cross section, τ_1 = lifetime of the first excited vibrational state, N_0 and N_1 = number of molecules in the vibrational ground and first excited state, n_L = number of laser photons per cm^2 and second, T = sample temperature, h = the Planck constant, and k = the Boltzmann constant. The first term in eq 3a describes the anti-Stokes signal due to thermal population of the first excited vibrational state. The second term, which shows a quadratic dependence on the excitation intensity, describes the contribution to the anti-Stokes signal that occurs due to vibrational pumping by the strong Stokes process. In normal Raman scattering, this term can be neglected since it is small compared to the thermal population. However, in SERS experiments at extremely high enhancement levels, this term is operative. Evidence for the pumping effect in the case of SERS comes from (i) anti-Stokes to Stokes signal ratios that cannot be explained in terms of a Boltzmann distribution and that are determined by the product of SERS cross section and vibrational lifetime and no longer by temperature,[10,17,19,20,22,23] (ii) a quadratic dependence of the anti-Stokes signal on the excitation intensity[17,23,24] (see also Figure 2), and (iii) a component of $\nu = 1$ to $\nu = 2$ Raman transitions in the Stokes signal in addition to the $\nu = 0$ to $\nu = 1$ transitions usually observed in Raman scattering.[17] To account for all these experimental observations, the product of cross section and vibrational lifetime in eq 3a must be on the order of 10^{-27} cm^2·s. Assuming vibrational lifetimes on the order of 10 ps, the surface-enhanced Raman cross section is then estimated to be at least $\sim 10^{-16}$ cm^2 per molecule.

At this point, it is important to clarify that for straightforward extraction of information on effective SERS cross sections, population pumping has to be studied under nonresonant Raman conditions to avoid a complex interference of resonance Raman[25−27] or temperature effects or both with the pumping effect. By applying near-infrared excitation at 830 nm, we inferred effective surface-enhanced Raman cross sections on the order of at least 10^{-16}cm^2 corresponding to SERS enhancement factors of 10^{14} for different kinds of molecules.[17,20,23] These nonresonant SERS enhancement factors were later confirmed in single-molecule Raman experiments.[18,19] Figure 3 shows Raman spectra measured from aqueous solution of silver nanoaggregates containing 10^{-14} M pseudoicocyanine (PIC) and 5 M methanol, which yields one PIC molecule and $\sim 10^{14}$ methanol molecules in the 30 pL probed volume. The experiment shows that the SERS signals of a single PIC molecule appears at the same signal level as the nonenhanced Raman signal of the 10^{14} methanol molecules. Raman lines assigned to PIC appear at varying signal levels due to Brownian motion of the silver colloidal cluster carrying single PIC molecules into and out of the probed volume.

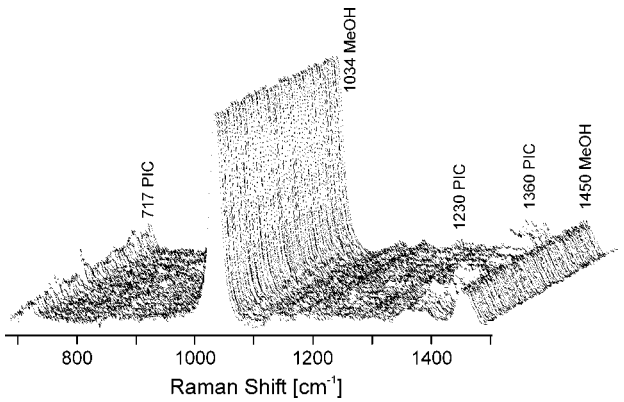

FIGURE 3. SERS spectra measured from a probed volume that contains one pseudoicocyanine (PIC) molecule attached to a silver colloidal cluster and $\sim 10^{14}$ methanol molecules.[19]

In principle, electromagnetic and chemical effects can account for the observed enhancement level on the order of 10^{14}. Theoretical estimates for different silver and gold nanostructures from dimers [28−30] to self-similar structures [31−33] show that local optical fields can give rise to SERS enhancement factors up to 10^{12}. This leaves a factor $10-10^3$ for an electronic contribution to match the experimentally observed enhancement factors in nonresonant SERS. However, the extent of electronic enhancement remains a subject of discussion. Recent studies show that combining plasmon resonances and photonic resonances can give rise to electromagnetic SERS enhancement factors sufficient for single-molecule SERS without chemical enhancement.[34] Other recent studies come back to chemical mechanisms involving ballistic electrons to explain extremely large SERS enhancement factors in single-molecule SERS.[35,36] A possible chemical contribution in SERS experiments might also be supported by the observation that there are molecules that do not show a SERS effect and also by a recent report claiming that small silver clusters consisting of a few silver atoms can result in strongly enhanced Stokes and anti-Stokes Raman signals.[37]

Isolated Nanoparticles vs Nanoaggregates. Figure 4 compares SERS experiments performed on isolated gold nanoparticles and on small aggregates formed by these spheres. In agreement with theory,[38,39] enhancement factors for isolated gold spheres have been estimated to be 10^3-10^4.[20] These SERS enhancement factors are too small to measurably populate the first excited vibrational state and the anti-Stokes spectrum appears at the ex-

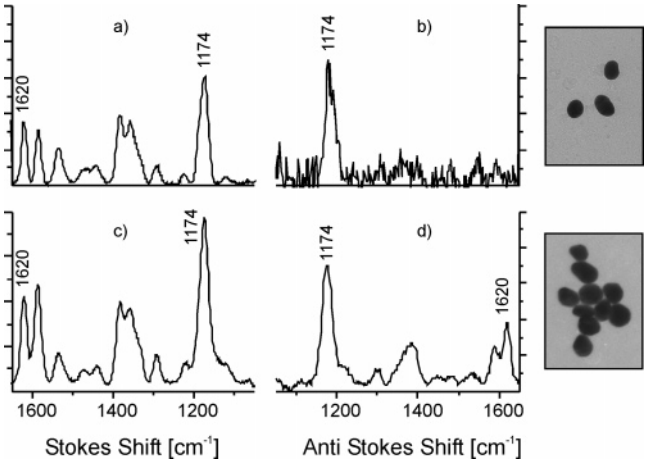

FIGURE 4. Stokes and anti-Stokes SERS spectra of crystal violet attached to isolated and aggregated gold nanospheres.

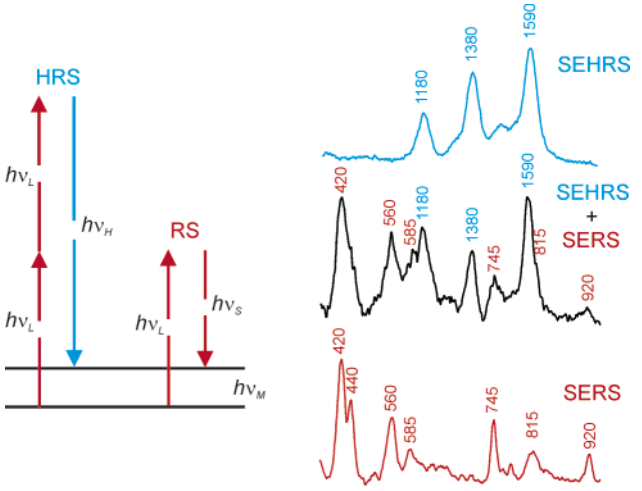

FIGURE 5. Schematic of hyper-Raman and Raman scattering and surface-enhanced Raman and hyper-Raman spectra of crystal violet on silver nanoclusters, excitation 850 nm, 10^7 W/cm^2.

pected relatively low signal level (Figure 4b). In particular, the high-frequency modes are not seen on the anti-Stokes side due to their low thermal population. This situation changes for SERS performed on cluster structures at 830 nm excitation (Figure 4d). Now a strong anti-Stokes signals appears, in particular also of higher frequency Raman modes. This is an indication of a very strong Raman process that populates the first excited vibrational state. As we have shown in the previous section, this vibrational pumping indicates nonresonant SERS enhancement factors on the order of 10^{14} or, in other words, a gap of 10 orders of magnitude between SERS enhancement factors for isolated gold nanoparticles and gold nanoclusters.[22] For silver nanoclusters, the SERS enhancement factor measured at 830 nm excitation has been experimentally found to be 7 orders of magnitude higher than enhancement factors for isolated silver colloidal particles, even when excited at their plasmon resonance at 407 nm. These experiments give evidence that extremely high enhancement factors and single-molecule sensitivity, at least in nonresonant SERS, are associated with the formation of clusters. Anti-Stokes to Stokes signal ratios measured on different clusters from 150 nm aggregates to larger fractal silver structures show that enhancement factors on the order of 10^{14} in nonresonant SERS are independent of the size and shape of the cluster.[20,22] Despite different SERS enhancement factors for isolated nanoparticles of silver (10^6–10^7) and gold (10^3–10^4) measured at their plasmon resonances at 407 and 514 nm, respectively, the enhancement factors for nanoclusters formed by these particles are on the same order of magnitude (10^{14}) for both metals.[22]

Field Confinement. The local optical fields on composites of nanoparticles such as clusters tend to be highly localized.[31–33] Near-field images taken on top of silver cluster structures confirm the existence of optical "hot spots" and "cold zones" on these structures.[40]

Since SERS takes place in the local fields of metallic nanostructures, the probed volume is determined by the confinement of the local fields, which can be 2 orders of magnitude better than the diffraction limit. The strongly confined "hot spots" provide the opportunity to spectroscopically select single nanoobjects or molecules within a larger population. This was demonstrated in SERS experiments performed on bundles of single-wall carbon nanotubes (SWNTs) on fractal silver cluster structures.[23] The spectroscopic selection of single SWNTs within a bundle of nanotubes shows that SERS signals are collected from dimensions smaller than 5 nm. It is interesting to compare SERS on the hot spots of nanoclusters with SERS exploiting local optical fields of metal tips used in atomic force microscopy.[41–43] Despite the high field confinement reported for these tips, which is comparable to the dimension in the hot spot on nanoclusters, enhancement factors of tips are reported to be orders of magnitude below those required for nonresonant single-molecule Raman spectroscopy.

Surface-Enhanced Nonlinear or Two-Photon Raman Scattering

Hyper-Raman scattering (HRS) is a nonlinear Raman process that results in an incoherent Raman signal shifted relative to the second harmonic of the excitation laser (see Figure 5). HRS follows symmetry selection rules different from Raman scattering, and therefore it can probe vibrations that are forbidden in Raman scattering.[44] However, HRS is an extremely weak effect. Cross sections on the order of 10^{-65} cm^4·s/photon make the utilization of HRS as a practical spectroscopic tool nearly impossible. In the framework of electromagnetic field enhancement, HRS particularly benefits from high local optical fields of nanoclusters because of its nonlinear dependence on the (enhanced) laser field.

Figure 5 displays surface-enhanced hyper-Raman scattering (SEHRS) and SERS spectra measured from crystal violet on silver nanoclusters using 850 nm excitation. The middle spectrum shows SEHRS and SERS measured in one spectrum by simultaneously using the first and second diffraction order of the spectrograph.[45] Despite the very different signal strengths of Raman and hyper-Raman

scattering, SERS and SEHRS spectra appear at the same signal level. This show that SEHRS must be enhanced at least 10^6 times more than SERS to compensate for the smaller cross section. The factor 10^6 can be understood considering the quadratic dependence of the effect on the enhanced local optical fields. Enhancement of field strengths on the order of 10^3 ($A(\nu_{L,S})$ in eq 1) yield electromagnetic enhancement factors on the order of 10^{12} for SERS and, due to the quadratic dependence, 10^6 times higher enhancement factor for SEHRS.[46]

Ultrasensitive Chemical Probing in Living Cells

The ability for very sensitive Raman detection, along with the fact that the spectral information in SERS only comes from the immediate vicinity of the nanostructures, makes gold and silver nanoprobes based on SERS ideal tools for targeted studies in living biological systems, in particular, the investigation of small morphological structures in cells. Gold nanoparticles have been tools of the trade in cell biology because of their favorable physical and chemical properties and biocompatibility.

We have been able to show that nanoparticulate structures from gold, while providing the local optical fields necessary for ultrasensitive probing, also fulfill the requirements posed by a cellular system.

Delivery of nanoparticles into the cellular interior, as well as routing of the particles or targeting of cellular compartments, can be achieved in various ways, depending on the nature of the experiment, but also on the type of cell line and physicochemical particle parameters, such as size, shape, and surface functionalization.[47−51] In our effort to develop Raman-based optical sensors to probe live cells, we have started to employ the fact that many cells take up nanostructures by themselves without further induction (Figure 6a). Nonphagocytic cells can internalize structures of less than 1 μm in size, with endocytosis and transport into late endosomes and lysosomes occurring for sizes up to 200 nm and highest efficiency for particles of several tens of nanometers.[48] This illustrates that the optimum size conditions for SERS enhancement can be in perfect agreement with the size requirements of nanoclusters employed in targeting of substructures that are involved in major transport pathways in the cells.

At positions in the cells where the gold nanostructures are present, surface-enhanced Raman spectra can be measured, enabling sensitive chemical probing of the particles' vicinity in very short times (≤1 s per spectrum) and low laser power (≤2 mW/1 μm spot) (Figure 6b). Such short acquisition times are on the order of the time scales of the processes occurring in a cell, enabling investigations that have been impossible so far in normal Raman experiments. Raman studies using laser powers low enough for living cells to withstand, unless they exploit molecule-selective resonance conditions,[52−54] usually require accumulation times on the order of a few minutes or even longer.[55,56] Typical SERS spectra from a living cell are shown in Figure 6b. They show features of the typical

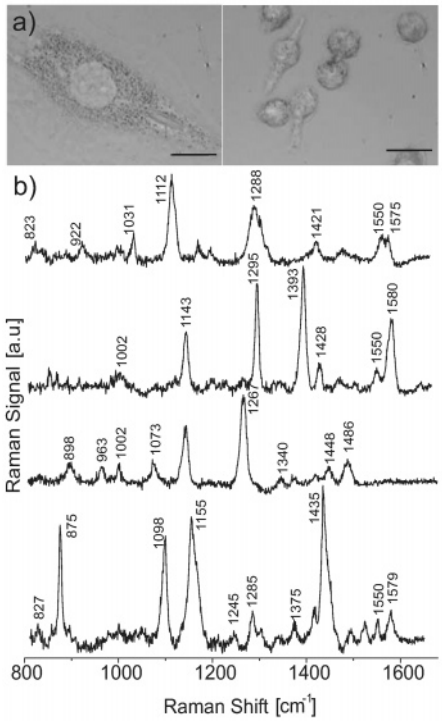

FIGURE 6. (a) Cells of a fibroblast cell line, NIH/3T3 (nonphagocytic) (left), and a macrophage cell line, J774 (phagocytic) (right), after uptake of gold nanoparticles; particle accumulations are visible as black dots inside the cells. Scale bars = 20 μm. (b) Examples of SERS spectra acquired from NIH/3T3 cells after 3 h incubation with gold nanostructures, excitation wavelength 830 nm, 1 s collection time.

cellular constitutents, such as proteins (1245 cm^{-1}, 1267 cm^{-1} amide III, side chains Phe 1002 cm^{-1}, Tyr 825 cm^{-1}) and various nucleic acid constituents (e.g. 1580, 1575, 1098 cm^{-1}), to mention a few.

It is also possible to attach a reporter molecule, for example, a dye, to the gold nanostuctures. Such probes can be localized inside single cells using the strong and distinct SERS signature of the attached reporter. In addition to its detection by the characteristic SERS spectrum of the reporter, the gold nanoparticle also delivers the SERS contribution from molecules and molecular groups in its vicinity.[57] Transferring reporter molecules together with the gold nanostructures into the cells will enable the identification of different nanostructure populations and ultrasensitive chemical probing of their respective nanoenvironments, that is, targeted multiplex vibrational characterization. Further, it may prove useful for spectroscopic observation of molecules that are transferred by the nanostructures, a question that is of particular interest for delivery of molecules, such as drugs.

Because of the important role of nanoaggregates and clusters for electromagnetic enhancement, controlling the formation of gold nanoparticle aggregates has been of extreme interest for further development of SERS probing in cell biological experiments. Results from electron microscopy studies of nanoparticles after immersing them in calf serum-containing culture medium suggest that apart from the individual particles, there occurs formation of stable nanoaggregates. We can conclude that the

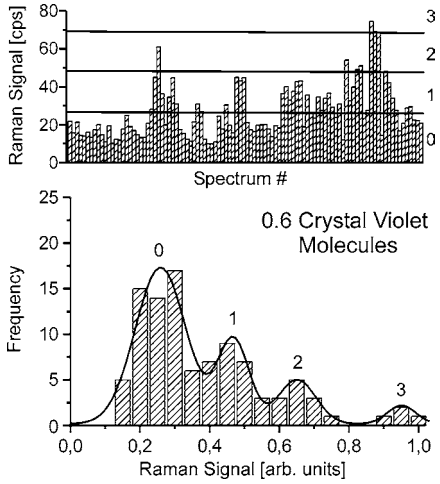

FIGURE 7. (a) Time sequence of the SERS signals of the 1174 cm^{-1} Raman line of crystal violet (CV) attached to silver nanoclusters in water using 830 nm excitation and (b) statistical analysis of 100 SERS measurements at an average of 0.6 CV molecules in the probed volume. The *x*-axis is divided into bins whose widths are 5% of the maximum signal. The *y*-axis displays the frequency of the appearance of the appropriate signal levels. The experimental data were fit by the sum of three Gaussian curves (solid line), whose areas' gradation is consistent with a Poisson distribution for an average number of 0.5 molecules.[18]

controlled generation of nanoaggregates will be one of our major tools to employ the large enhancement factors of such structures in live biosystems.

Single-Molecule SERS Spectroscopy on Nanoclusters—Why Does It Work so Well?

So far, silver and gold nanoaggregate cluster structures formed by individual nanoparticles between 20 and 60 nm in size were found to exhibit the best SERS enhancement factors of 10^{14} and allow Raman measurements of single molecules under molecular nonresonant conditions. Single-molecule Raman spectra are observed also at the anti-Stokes side of the excitation laser.[18,19] Effective SERS cross sections on the order of 10^{-16} cm^2 give rise to measurable vibrational pumping that reveals itself in unexpectedly strong anti-Stokes signals.[17]

The high local optical fields in the hot spots of silver and gold cluster structures provide a rationale for this level of SERS enhancement.[10−12] The scaling between enhancement factors observed for one-photon SERS and two-photon excited SEHRS provides further indications for the dominating role of the electromagnetic mechanism.[46]

In general, the field enhancement in the hot spots is extremely sensitive to the distance of the particles, as well as the frequency and polarization of the excitation laser.[29−40] This explains that small clusters comprising 2−3 individual particles can fail to provide a hot spot for the applied light resulting in "hot" and "cold" nanoclusters.[21] We found that clusters exceeding a size of 100−150 nm and consisting of a minimum of 5−10 individual nanoparticles provide at least one hot spot exhibiting an enhancement at a level that makes these nanostrutures SERS-active for nonresonant single-molecule Raman detection.

Figure 7 shows SERS signals of crystal violet measured from a sample of single crystal violet molecules attached to small silver nanoclusters in water. Brownian motion of these clusters in to and out of the probed volume results in strong statistical changes in SERS signals measured from such a sample in time sequence. The Poisson distribution of the Raman signal reflects the probability of finding zero, one, two, or three molecules in the scattering volume.

The uniform enhancement in the hot spots of a cluster on the order of 10^{14} [20,22,39] explains the relatively well quantized SERS signals for one, two, and three molecules in the probed volume and allows counting of single molecules.

The strong local confinement of the hot spots results in large field gradients that force molecules to go to this spot and to stay there. The experiments show that in a highly dilute solution of analyte molecules and small gold or silver clusters (concentration of the analyte less than the concentration of the small clusters) more than 80% of the analyte molecules find a hot spot and are detected. This can be concluded from the good agreement of the Poisson statistics with the number of molecules in the probed volume known from concentration and focal volume.

The mainly electromagnetic origin of the extremely large SERS enhancement suggests silver and gold nanoaggregates for nonresonant single-molecule Raman detection for a wide range of molecules. The favorable enhancing properties along with their biocompatibility make such gold nanostructures very promising tools for ultrasensitive chemical probing in live cells.[57]

This work is supported in part by DOD Grant No. AFOSR FA9550-04-1-0079 and by the generous gift of Dr. and Mrs. J. S. Chen to the optical diagnostics program of the Massachusetts General Hospital Wellman Center for Photomedicine.

References

(1) Fleischman, M.; Hendra, P. J.; McQuillan, A. J. Raman-Spectra of Pyridine Adsorbed at a Silver Electrode. *Chem. Phys. Lett.* **1974**, *26*, 163−166.
(2) Jeanmaire, D. L.; Duyne, R. P. V. Surface Raman Spectroelectrochemistry. 1. Heterocyclic, Aromatic, and Aliphatic-Amines Adsorbed on Anodized Silver Electrode. *J. Electroanal. Chem.* **1977**, *84*, 1−20.
(3) Albrecht, M. G.; Creighton, J. A. Anomalously Intense Raman Spectra of Pyridine at a Silver Electrode. *J. Am. Chem. Soc.* **1977**, *99*, 5215−5217.
(4) Creighton, J. A.; Blatchford, C. G.; Albrecht, M. G. Plasma Resonance Enhancement of Raman-Scattering by Pyridine Adsorbed on Silver or Gold Sol Particles of Size Comparable to the Excitation Wavelength. *J. Chem. Soc., Faraday Trans II* **1979**, *75*, 790−798.
(5) Moskovits, M. Surface roughness and the enhanced intensity of Raman scattering by molecules adsorbed on metals. *J. Chem. Phys.* **1978**, *69*, 1459−1461.
(6) Otto, A. In *Light scattering in solids IV. Electronic scattering, spin effects, SERS and morphic effects*; Cardona, M., Guntherodt, G., Eds.; Springer-Verlag: Berlin, Germany, 1984; Vol. 1984, pp 289−418.
(7) Persson, B. N. J. On the theory of surface-enhanced Raman scattering. *Chem. Phys. Lett.* **1981**, *82*, 561−565.
(8) Moskovits, M. Surface-enhanced spectroscopy. *Rev. Mod. Phys.* **1985**, *57*, 783−826.
(9) Kambhampati, P.; Child, C. M.; Foster, M. C.; Campion, A. On the chemical mechanism of surface enhanced Raman scattering: experiment and theory. *J. Chem. Phys.* **1998**, *108*, 5013−5026.

(10) Kneipp, K.; Kneipp, H.; Itzkan, I.; Dasari, R. R.; Feld, M. S. Ultrasensitive Chemical Analysis by Raman Spectroscopy. *Chem. Rev.* **1999**, *99*, 2957−2975.
(11) Kneipp, K.; Kneipp, H.; Itzkan, I.; Dasari, R. R.; Feld, M. S. Surface-enhanced Raman scattering and biophysics. *J. Phys.: Condens. Matter* **2002**, *14*, R597−R624.
(12) Moskovits, M. Surface-enhanced Raman spectroscopy: a brief retrospective. *J. Raman Spectrosc.* **2005**, *36*, 485−496.
(13) Hildebrandt, P.; Stockburger, M. Surface-Enhanced Resonance Raman Spectroscopy of Rhodamine 6G Adsorbed on Colloidal Silver. *J. Phys. Chem.* **1984**, *88*, 5935−5944.
(14) Pettinger, B.; Krischer, K. Comparison of Cross-Sections for Absorption and surface-enhanced resonance Raman Scattering for Rhodamine 6G at Coagulated Silver Colloids. *J. Electron Spectrosc. Relat. Phenom.* **1987**, *45*, 133−142.
(15) Kneipp, K. High-Sensitive SERS on Colloidal Silver Particles in Aqueous Solution. *Exp. Tech. Phys. (Berlin)* **1988**, *36*, 161−166.
(16) Kneipp, K.; Wang, Y.; Dasari, R. R.; Feld, M. S. Approach to Single Molecule Detection Using Surface-Enhanced Resonance Raman Scattering (SERRS): A Study Using Rhodamine 6G on Colloidal Silver. *Appl. Spectrosc.* **1995**, *49*, 780−784.
(17) Kneipp, K.; Wang, Y.; Kneipp, H.; Itzkan, I.; Dasari, R. R.; Feld, M. S. Population Pumping of Ecited Vibrational States by Spontaneous Surface-Enhanced Raman Scattering. *Phys. Rev. Lett.* **1996**, *76*, 2444−2447.
(18) Kneipp, K.; Wang, Y.; Kneipp, H.; Perelman, L. T.; Itzkan, I.; Dasari, R. R.; Feld, M. S. Single Molecule Detection Using Surface-Enhanced Raman Scattering (SERS). *Phys. Rev. Lett.* **1997**, *78*, 1667−1670.
(19) Kneipp, K.; Kneipp, H.; Deinum, G.; Itzkan, I.; Dasari, R. R.; Feld, M. S. Single-Molecule Detection of a Cyanine Dye in Silver Colloidal Solution Using Near-Infrared Surface-Enhanced Raman Scattering. *Appl. Spectrosc.* **1998**, *52*, 175−178.
(20) Kneipp, K.; Kneipp, H.; Kartha, V. B.; Manoharan, R.; Deinum, G.; Itzkan, I.; Dasari, R. R.; Feld, M. S. Detection and identification of a single DNA base molecule using surface-enhanced Raman scattering (SERS). *Phys. Rev. E* **1998**, *57*, R6281−R6284.
(21) Nie, S.; Emory, S. R. Probing single molecules and single nanoparticles by surface- enhanced Raman scattering. *Science* **1997**, *275*, 1102−1106.
(22) Kneipp, K.; Kneipp, H.; Manoharan, R.; Hanlon, E. B.; Itzkan, I.; Dasari, R. R.; Feld, M. S. Extremely Large Enhancement Factors in Surface-Enhanced Raman Scattering for Molecules on Colloidal Gold Clusters. *Appl. Spectrosc.* **1998**, *52*, 1493−1497.
(23) Kneipp, K.; Kneipp, H.; Corio, P.; Brown, S. D. M.; Shafer, K.; Motz, J.; Perelman, L. T.; Hanlon, E. B.; Marucci, A.; Dresselhaus, G.; Dresselhaus, M. S. Surface-enhanced and normal Stokes and anti-Stokes Raman spectroscopy of single-walled carbon nanotubes. *Phys. Rev. Lett.* **2000**, *84*, 3470−3473.
(24) Teredesai, P. V.; Sood, A. K.; Govindaraj, A.; Rao, C. N. R. Surface enhanced resonance Raman scattering from radial and tangential modes of semiconducting single wall carbon nanotubes. *Appl. Surf. Sci.* **2001**, *182*, 196−201.
(25) Haslett, T. L.; Tay, L.; Moskovits, M. *J. Chem. Phys.* **2000**, *113*, 1641−1646.
(26) Brolo, A. G.; Sanderson, A. C.; Smith, A. P. Ratio of the surface-enhanced anti-Stokes scattering to the surface-enhanced Stokes-Raman scattering for molecules adsorbed on a silver electrode. *Phys. Rev. B* **2004**, *69*, No. 045424.
(27) Maher, R. C.; Cohen, L. F.; Etchegoin, P.; Hartigan, H. J. N.; Brown, R. J. C.; Milton, M. J. T. Stokes/anti-Stokes anomalies under surface enhanced Raman scattering conditions. *J. Chem. Phys.* **2004**, *120*, 11746−11753.
(28) Metiu, H. In *Proceedings of the VIIth International Conference on Raman Spectroscopy. Linear and Non Linear Processes*; Murphy, W. F., Ed.; North-Holland: Amsterdam, Netherlands. 1980; pp 382−384.
(29) Inoue, M.; Ohtaka, K. Surface enhanced Raman scattering by metal spheres. I. Cluster effect. *J. Phys. Soc. Jpn.* **1983**, *52*, 3853−3864.
(30) Xu, H. X.; Bjerneld, E. J.; Kall, M.; Borjesson, L. Spectroscopy of single hemoglobin molecules by surface enhanced Raman scattering. *Phys. Rev. Lett.* **1999**, *83*, 4357−4360.
(31) Stockman, M. I.; Shalaev, V. M.; Moskovits, M.; Botet, R.; George, T. F. Enhanced Raman scattering by fractal clusters: Scale-invariant theory. *Phys. Rev. B* **1992**, *46*, 2821−2830.
(32) Shalaev, V. M. Electromagnetic Properties of Small-Particle Composites. *Phys. Rep.* **1996**, *272*, 61−137.
(33) Markel, V. A.; Shalaev, V. M.; Zhang, P.; Huynh, W.; Tay, L.; Haslett, T. L.; Moskovits, M. Near-field optical spectroscopy of individual surface-plasmon modes in colloid clusters. *Phys. Rev. B* **1999**, *59*, 10903−10909.
(34) Zou, S. L.; Schatz, G. C. Silver nanoparticle array structures that produce giant enhancements in electromagnetic fields. *Chem. Phys. Lett.* **2005**, *403*, 62−67.
(35) Michaels, A. M.; Nirmal, M.; Brus, L. E. Surface enhanced Raman spectroscopy of individual rhodamine 6G molecules on large Ag nanocrystals. *J. Am. Chem. Soc.* **1999**, *121*, 9932−9939.
(36) Otto, A. The 'chemical' (electronic) contribution to surface-enhanced Raman scattering. *J. Raman Spectrosc.* **2005**, *36*, 497−509.
(37) Capadona, L. P.; Zheng, J.; Gonzalez, J. I.; Lee, T. H.; Patel, S. A.; Dickson, R. M. Nanoparticle-free single molecule anti-stokes Raman spectroscopy. *Phys. Rev. Lett.* **2005**, *94*, No. 058301.
(38) Wang, D. S.; Chew, H.; Kerker, M. Enhanced Raman scattering at the surface (SERS) of a spherical particle. *Appl. Opt.* **1980**, *19*, 2256−2257.
(39) Kerker, M. Estimation of surface-enhanced Raman scattering from surface-averaged electromagnetic intensities. *J. Colloid Interface Sci.* **1987**, *18*, 417−421.
(40) Zhang, P.; Haslett, T. L.; Douketis, C.; Moskovits, M. Mode localization in self-affine fractal interfaces observed by near-field microscopy. *Phys. Rev. B* **1998**, *57*, 15513−15518.
(41) Hayazawa, N.; Inouye, Y.; Sekkat, Z.; Kawata, S. Metallized tip amplification of near-field Raman scattering. *Opt. Commun.* **2000**, *183*, 333−336.
(42) Hartschuh, A.; Sanchez, E. J.; Xie, X. S.; Novotny, L. High-resolution near-field Raman microscopy of single-walled carbon nanotubes. *Phys. Rev. Lett.* **2003**, *90*, No. 095503.
(43) Pettinger, B.; Ren, B.; Picardi, G.; Schuster, R.; Ertl, G. Nanoscale probing of adsorbed species by tip-enhanced Raman spectroscopy. *Phys. Rev. Lett.* **2004**, *92*, No. 096101.
(44) Denisov, V. N.; Mavrin, B. N.; Podobedov, V. B. Hyper Raman Scattering. *Phys. Rep.* **1987**, *151*, 1−92.
(45) Kneipp, H.; Kneipp, K.; Seifert, F. Surface-enhanced hyper-Raman scattering (SEHRS) and surface-enhanced Raman scattering (SERS) by means of mode-locked Ti:sapphire laser excitation. *Chem. Phys. Lett.* **1993**, *212*, 374−378.
(46) Kneipp, K.; Kneipp, H.; Itzkan, I.; Dasari, R. R.; Feld, M. S.; Dresselhaus, M. S. Nonlinear Raman probe of single molecules attached to colloidal silver and gold clusters. In *Optical Properties of Nanostructured Random Media*; Shalaev, V. M., Ed.; Springer: Berlin, 2002; Vol. 82, pp 227−247.
(47) Limbach, L. K.; Li, Y.; Grass, R. N.; Brunner, T. J.; Hintermann, M. A.; Muller, M.; Gunther, D.; Stark, W. J. Oxide Nanoparticle Uptake in Human Lung Fibroblasts: Effects of Particle Size, Agglomeration, and Diffusion at Low Concentrations. *Environ. Sci. Technol.* **2005**, *39*, 9370−9376.
(48) Rejman, J.; Oberle, V.; Zuhorn, I. S.; Hoekstra, D. Size-dependent internalization of particles via the pathways of clathrin- and caveolae-mediated endocytosis. *Biochem. J.* **2004**, *377*, 159−169.
(49) Arlein, W. J.; Shearer, J. D.; Caldwell, M. D. Continuity between wound macrophage and fibroblast phenotype: analysis of wound fibroblast phagocytosis. *Am. J. Physiol.* **1998**, *44*, R1041−R1048.
(50) Tkachenko, A. G.; Xie, H.; Liu, Y. L.; Coleman, D.; Ryan, J.; Glomm, W. R.; Shipton, M. K.; Franzen, S.; Feldheim, D. L. Cellular trajectories of peptide-modified gold particle complexes: Comparison of nuclear localization signals and peptide transduction domains. *Bioconjugate Chem.* **2004**, *15*, 482−490.
(51) Feldherr, C.; Kallenbach, E.; Schultz, N. Movement of a karyophilic protein through the nuclear pores of oocytes. *J. Cell Biol.* **1984**, *99*, 2216−2222.
(52) Sijtsema, N. M.; Otto, C.; Segers-Nolten, G. M. J.; Verhoeven, A. J.; Greve, J. Resonance Raman Microspectroscopy of Myeloperoxidase and Cytochrome b558 in Human Neutrophilic Granulocytes. *Biophys. J.* **1998**, *74*, 3250−3255.
(53) Wood, B. R.; Tait, B.; McNaughton, D. Micro-Raman characterisation of the R to T state transition of haemoglobin within a single living erythrocyte. *Biochim. Biophys. Acta* **2001**, *1539*, 58−70.
(54) Feofanov, A. V.; Grichine, A. I.; Shitova, L. A.; Karmakova, T. A.; Yakubovskaya, R. I.; Egret-Charlier, M.; Vigny, P. Confocal Raman Microspectroscopy and Imaging Study of Theraphthal in Living Cancer Cells. *Biophys. J.* **2000**, *78*, 499−512.
(55) Puppels, G. J.; De Mul, F.; Otto, C.; Greve, J.; RobertNicoud, M.; Arndt-Jovin, D. J.; Jovin, T. Studying single living cells and

chromosomes by confocal Raman microspectroscopy. *Nature* **1990**, *347*, 301−303.

(56) Peticolas, W. L.; Patapoff, T. W.; Thomas, G. A.; Postlewait, J.; Powell, J. W. Laser Raman microscopy of chromosomes in living eukaryotic cells: DNA polymorphism in vivo. *J. Raman Spectrosc,* **1996**, *27*, 571−578.

(57) Kneipp, J.; Kneipp, H.; Rice, W. L.; Kneipp, K. Optical probes for biological applications based on surface enhanced Raman scattering from indocyanine green on gold nanoparticles. *Anal. Chem.* **2005**, *77*, 2381−2385.

AR050107X